PHYSICAL REVIEW A VOLUME 24, NUMBER 2 AUGUST 1981

Measurements of total scattering cross sections for intermediate-energy positrons and electrons colliding with helium, neon, and argon

W. E. Kauppila, T. S. Stein, J. H. Smart,* M. S. Dababneh, Y. K. Ho, J. P. Downing, and V. Pol
Department of Physics, Wayne State University, Detroit, Michigan 48202
(Received 28 August 1979; revised manuscript received 17 April 1981)

Total scattering cross sections have been measured in the same apparatus for positrons and electrons colliding with helium, neon, and argon atoms in the energy range from 15 to 800 eV using a beam-transmission technique. These measurements reveal a merging of the positron and electron cross-section curves for helium at energies above 200 eV while the available theories predict this merging to occur at considerably higher energies. For neon and argon the positron and electron total-cross-section curves are slowly approaching each other at the highest energies. The present experimental approach is analyzed with regard to the discrimination against small-angle forward elastic scattering, and estimates are made of other potential errors in the measured total cross sections. The present results are used to test the zero-energy sum rule, obtained from forward dispersion relations, and it is found that these data are consistent with prior measurements in that the sum rule is found to fail for electron scattering and to be valid for positron scattering.

I. INTRODUCTION

During recent years, there has been considerable interest in measuring total cross sections for the scattering of positrons and electrons by the simpler inert gas atoms to provide tests of various theoretical approximations. Positron-beam experiments, which have only begun in the present decade and have recently been the subject of a review article by Griffith and Heyland,[1] are of particular interest because they can provide a very sensitive test of the theories that have been developed for electron-atom scattering.[2] Since the positron is distinguishable from the electrons in the target atoms, there is no exchange interaction for positrons. Meanwhile, the static interaction is repulsive for positrons, while it is attractive for electrons. The polarization interaction is attractive for both particles. These differences and similarities manifest themselves in some interesting ways when comparisons are made between the scattering of positrons and electrons by atoms. At low energies the static and polarization interactions will tend to cancel each other for positron scattering, while these interactions add for electron impact. At sufficiently high energies, only the static interaction will remain, with the result being that the total scattering cross sections will be the same for positrons and electrons, and will be given by the first Born approximation. Two phenomena that can only occur for positron collisions are annihilation (appreciable only for energies much less than 1 eV) and positronium formation, both real and "virtual".

In the low-energy region, below the lowest inelastic threshold, there has been much experimental and theoretical work for electrons and positrons colliding with helium. For e^--He scattering at energies below the first excitation threshold (19.8 eV) several recent experiments,[3-5] using different approaches, are found to be in excellent agreement (better than ±5%) with each other and with the theories of Sinfailam and Nesbet,[6] Callaway *et al.*,[7] O'Malley *et al.*,[8] and Nesbet.[9] Meanwhile, the situation for low-energy e^+-He scattering is not as clear since there is some disagreement between the total-cross-section measurements of Canter *et al.*,[10] Jaduszliwer and Paul,[11] Stein *et al.*,[12] Burciaga *et al.*,[13] and Wilson.[14] A theoretical calculation by Campeanu and Humberston,[15] considered to be the best for e^+-He scattering, appears to be in agreement with the work of Canter *et al.*[10] The experiments of Stein *et al.*[12] and Burciaga *et al.*[13] agree with each other and with the theory[15] above 6 eV, but are lower than theory[15] below 6 eV. It has been suggested by Humberston[16] that this discrepancy may be due to the inability of the experiments of Stein *et al.*[12] and Burciaga *et al.*[13] to effectively discriminate against all of the positrons undergoing small-angle forward scattering. The normalized measurements of Wilson[14] are somewhat higher than the Campeanu and Humberston calculations[15] and the results of Jaduszliwer and Paul[11] are considerably higher than the same calculations. The work of Stein *et al.*[12] clearly demonstrates the existence of a Ramsauer-Townsend effect (a minimum in the total scattering cross section) for e^+-He collisions in the vicinity of 2 eV.

In the case of low-energy positron and electron scattering by neon and argon, the overall picture is less clear than for helium due to the increased

complexity of the scattering systems. The present situation for positrons is adequately discussed by Griffith and Heyland[1] with there being some significant discrepancies between the various experimental measurements. Ramsauer-Townsend effects have been observed for positrons incident on neon[12] and argon[17] in the vicinity of 0.6 and 2.0 eV, respectively. For e^--Ne, Ar collisions, the various experiments are in better agreement than for positron scattering, as can be seen in the papers by Kauppila *et al.*[4] and Stein *et al.*[12]

There is currently considerable interest in determining cross sections for positrons and electrons colliding with atoms at intermediate energies, which extend from the thresholds of inelastic collision processes up to the energy region where the first Born approximation should describe the scattering. In recent review articles Bransden and McDowell[18] and Byron and Joachain[19] discuss various theoretical approaches that are being used to calculate these intermediate-energy cross sections. Griffith and Heyland,[1] in discussing the intermediate-energy positron-He, Ne, and Ar total-cross-section measurements, which are not in particularly good agreement (except for a rather limited energy range in helium), point out that these measurements have been and may still be affected by an inability to discriminate against all of the inelastically scattered positrons and the positrons elastically scattered through small angles in the forward direction. The 200–1000 eV positron-helium total-cross-section measurements of Brenton *et al.*[20] are in good agreement with the "distorted-wave second Born approximation" (DWSBA) calculation of Dewangen and Walters,[21] while the total e^--He cross-section measurements of Blaauw *et al.*[22] are in agreement with the Born approximation given by de Heer *et al.*[23] for energies above 200 eV. For positrons and electrons colliding with neon and argon, there are no similar indications of agreement between theory and experiment for total scattering cross sections.

Another aspect of total scattering of positrons and electrons by atoms that has received considerable attention in recent years is the question concerning the validity of the sum rule,[24] which is based on the forward dispersion relations of Gerjuoy and Krall.[25] For scattering by the inert gases, in which the projectile and the target atoms do not form bound states, the sum rule has the form

$$-a - f_B^D + f_B^E = \frac{1}{2\pi}\int_0^\infty Q_t(k)dk, \qquad (1)$$

where a is the scattering length, f_B^D and f_B^E are the first Born amplitudes for elastic direct and exchange scattering, respectively, and $Q_t(k)$ is the total scattering cross section expressed as a function of the momentum k. Both the scattering length and the zero-energy scattering amplitudes are expressed in units of a_0, the Bohr radius, and the total cross section $Q_t(k)$ is in units of πa_0^2. By using available total-cross-section measurements for positrons and electrons scattering from helium (for energies up to where the Born approximation is considered to be valid) to evaluate the integral in Eq. (1) and theoretical results for the other terms in Eq. (1), it is now apparent[20,23,26-29] that the sum rule is valid when applied to e^+-He scattering and not valid for e^--He scattering. The differing results for positrons and electrons are understood[23,28-30] to arise from the nature of singularities in the exchange amplitude, which causes the sum rule to fail for electron scattering. No such difficulties arise in positron collisions since there are no exchange effects involved between the incoming positron and target electrons.

Tests of the sum rule for positrons and electrons scattering from neon and argon are not as straightforward as for helium due to the greater uncertainty in evaluating a, f_B^D, and f_B^E from the theory, and the fact that the measured total cross sections at the highest energies do not yet merge with the Born approximation results. The available evidence[26,29,31] indicates a similar situation as is found for helium, in that the sum rule appears to be valid for positron scattering and not valid for electron scattering.

In this paper, we report total-cross-section measurements for intermediate-energy positrons and electrons colliding with helium, neon, and argon atoms. The comparisons that are made between the electron and positron results should be particularly meaningful because they represent the first measurements made with the same experimental apparatus and technique at these energies. An effect that could alter these comparisons is an inability to discriminate against all small-angle forward elastic scattering, which is different for positron and electron impact for energies below those at which the Born approximation is valid. The angular discrimination of the present experiment is analyzed in Sec. III and estimates are made of the corresponding potential errors in the measured total cross sections, which are presented in Sec. IV. Other potential experimental errors in the absolute total-cross-section measurements and in the positron and electron comparison measurements are discussed

in Sec. V. The use of the present results to test the sum rule is discussed in Sec. VI.

II. EXPERIMENTAL APPARATUS AND PROCEDURE

Detailed discussions of the apparatus and procedure used in the present measurements have appeared elsewhere[4,12,32,33] and only a brief overview will be presented here. A schematic diagram of the experimental apparatus is shown in Fig. 1. A Van de Graaff accelerator is used to generate an ^{11}C positron source by the reaction $^{11}B(p,n)^{11}C$. A variable-energy positron beam having an energy width of less than 0.1 eV is produced and guided by a weak, axial magnetic field through a curved, differentially pumped gas scattering region to the detector, a channeltron electron multiplier (CEM). For the electron measurements, the positron source is replaced by a thermionic electron source (type B Philips cathode).

Total cross sections for positrons and electrons colliding with gases are determined by measuring the attenuation of the projectile beam as it passes through the gas scattering region. The transmitted beam current, under "ideal" conditions, is given by

$$I = I_0 e^{-nQ_T L}, \tag{2}$$

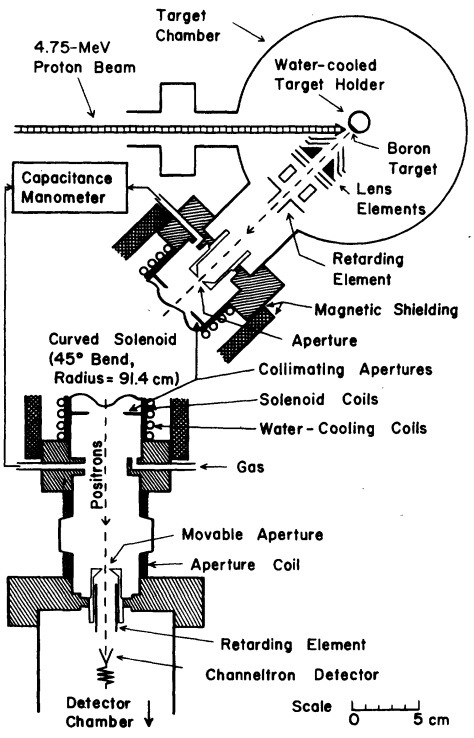

FIG. 1. Schematic diagram of the apparatus.

where n is the target-gas number density in the scattering region, L is the path length of the beam through the scattering region, Q_T is the total scattering cross section, and I_0 is the detected beam current with no gas in the scattering region. The target-gas number density n is determined from the measured pressure and temperature of the gas in the scattering region, while the path length L is taken as the axial distance (109 cm) between the gas-confining apertures of the scattering region. Both I and I_0 are corrected for "spurious" CEM counts and the small number of detected positrons having energies higher than the desired narrow-energy-width positron beam. Signal-to-noise ratios for the positron beams used in this work were generally larger than 100:1 and sometimes were as large as 1000:1, while the ratios were even better for the detected electron beams (typically greater than 500:1). The "noise" count rates were determined by stopping the primary beam with a retarding potential that was generally 1 V higher than the voltage applied to the source for electrons at all energies, while the "stopping" potentials used for positrons were generally 1 V higher for $E<100$ eV and 2 V higher for $E>100$ eV. The energies of the positron and electron beams were established by the voltage applied to the source and retarding potential measurements were used to assign the absolute energy.

A routine step in the procedure is to measure the total cross section at each energy for varying gas number densities in the scattering region, to insure that I vs I_0 has the proper exponential dependence, as given by Eq. (2). Another important aspect of the procedure is the use of a retarding potential element, located after the scattering region, to discriminate against (1) all of the positrons and electrons which have participated in inelastic collision processes and (2) some of the positrons and electrons which were elastically scattered. Discrimination against the elastically scattered projectiles becomes increasingly more difficult as the angle of scattering in the forward direction decreases. As a result, the discrimination against elastically scattered projectiles is incomplete and will depend on several experimental parameters and various effects discussed in Secs. III and IV.

III. DISCRIMINATION AGAINST PROJECTILES ELASTICALLY SCATTERED AT SMALL FORWARD ANGLES

Elastic scattering of positrons and electrons by atoms is characterized by the scattered pro-

jectile particle having very nearly the same energy as its incident energy. For elastic scattering at small angles in the forward direction, the degree of discrimination depends on the angle of scattering and on the nature of the experimental apparatus and approach. In the present experiment, this discrimination is provided by a combination of (1) the retarding potential that is applied to an element following the scattering region and preceding the detector and (2) the size of the beam exit aperture from the gas scattering region.

A. Effect of the retarding potential procedure

In order to provide discrimination against beam particles elastically scattered in the forward direction, we have made use of a retarding potential element located between the gas-confining exit aperture and the CEM detector (see Fig. 1). For each projectile energy studied, the potential applied to this retarding element is set (with the scattering region evacuated) so as to decrease the beam intensity to 80% of the beam intensity with no applied retarding potential. As described elsewhere,[4] the steepest portion of the retarding potential curve is at the voltages immediately above the retarding potential value that gives an 80% beam transmission. When a particle undergoes elastic scattering, some energy associated with axial motion is transferred to energy associated with transverse motion. Since the retarding potential element retards only the axial component of velocity, a particle of incident energy E, which scatters at an angle θ_S in the forward direction, may lose sufficient energy associated with axial motion, $E - E\cos^2\theta_S = E\sin^2\theta_S$, that it will no longer be able to surmount the retarding potential barrier.

An estimate of the angular discrimination (the smallest angle of scattering in the forward direction that can be discriminated against) obtained with the retarding potential approach can now be made. For a "median" energy detected projectile beam particle, one that will be on the verge of being stopped when the retarding potential element transmits only 40% of the beam, the angular discrimination is determined from the expression

$$E_{40} - E_{80} = E\sin^2\theta_S\,, \tag{3}$$

where E_{40} and E_{80} correspond to the energies of incident projectile beam particles that are on the verge of being stopped when the retarding potential element passes 40% and 80% of the beam.

The expression for the angular discrimination, Eq. (3), applies only when both the scattering and retarding occur in either a region free of any magnetic fields or a region having a uniform axial magnetic field. In the present experiment a nonuniform axial magnetic field is used, with the field in approximately 90% of the scattering region being determined by the curved solenoid and the field at the retarding element being determined by the current-carrying coil surrounding the exit aperture from the scattering region. As a result, the angle between the direction of motion of the scattered projectile and the axial direction will change depending on the magnitude of the axial magnetic field. It is well known[34] that for a charged particle moving at some angle θ to a slowly varying axial magnetic field B,

$$p_\perp^2/B = \text{const}\,, \tag{4}$$

where $p_\perp$ is the component of momentum of the particle perpendicular to the axial direction of the magnetic field. By expressing $p_\perp$ in terms of the total momentum, $p_\perp = p\sin\theta$, one obtains the following expression relating the angle θ with the field B at different points:

$$(\sin^2\theta_1)/B_1 = (\sin^2\theta_2)/B_2\,. \tag{5}$$

From Eqs. (3) and (5), one gets the expression for the angular discrimination for a beam particle with median energy E $(=E_{40})$ as

$$\theta_S(R) = \arcsin(B_S\Delta E/B_R E)^{1/2}\,, \tag{6}$$

where B_S and B_R are the magnetic-field strengths in the scattering region (assumed uniform throughout) and at the retarding element, and $\Delta E = E_{40} - E_{80}$.

B. Effect of the beam exit aperture

The beam exit aperture from the scattering region provides discrimination against elastically scattered projectiles in that after the projectile is scattered at some angle to the axial beam-confining magnetic field (assuming it was initially moving parallel to the field) the scattered projectile will acquire spiralling motion which will decrease its probability of passing through the exit aperture leading to the detector. This discrimination will depend on the nature of the unscattered projectile beam (energy, and spatial and velocity distributions), the aperture, and the distribution of angles at which the elastic scattering occurs.

A reasonable estimate of the discrimination provided by this effect can be made with some simplifying assumptions. It is assumed that the unscattered primary beam is moving parallel to the axial magnetic field at the aperture and that the entire beam passes through the aperture and has a uniform spatial distribution throughout the cross-sectional area of the aperture. (These are

reasonable assumptions because of the manner by which the primary beam is initially tuned to provide the highest detected beam intensity consistent with the narrowest attainable beam energy distribution, and the use of the smallest magnetic fields in the scattering region and at the detector aperture.) When gas is introduced into the scattering region, projectiles scattered at an angle θ_S to their original direction of motion will begin spiralling with an orbit radius of

$$r = mv(\sin\theta_S)/qB, \tag{7}$$

where m, q, and v are the mass, charge, and speed of the projectile, and B is the magnetic-field strength. As the size of the orbit radius increases relative to the size of the aperture, the scattered projectile is less likely to pass through the aperture and be detected. The results of a calculation that has been performed to determine the transmission fraction of the scattered projectile particles versus their orbital radii at the exit aperture are shown in Fig. 2. The final consideration that is necessary to enable an estimate of the discrimination is the variation of the magnetic-field strength from the scattering region to the exit aperture. If the magnetic field varies at a sufficiently slow rate the magnetic flux through the projectile's orbit,

$$B\pi r^2 = \text{const}. \tag{8}$$

As a result, the orbit radius varies as the projectile travels from the scattering region (denoted by subscript S) to the exit aperture (denoted by subscript A) and is given by

$$B_S r_S^2 = B_A r_A^2. \tag{9}$$

From Eqs. (7) and (9), one obtains the relationship

$$\theta_S(A) = \arcsin[qr_A(B_A B_S/2mE)^{1/2}], \tag{10}$$

which relates the orbit radius at the exit aperture to the angle of scattering of the projectile in the scattering region. From Fig. 2 we find that if all the projectiles are scattered such that their orbital radii are 65% of the aperture radius ($R_A = 2.38$ mm; $r_A = 1.55$ mm) then 50% of the scattered projectiles would not pass through the aperture. This value for the orbit radius will be used in the following discussion to estimate the angular discrimination resulting from the exit aperture size.

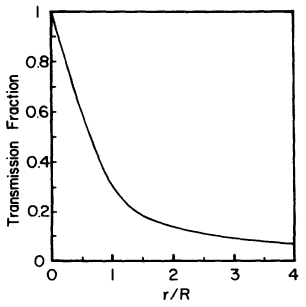

FIG. 2. Calculated fraction of scattered projectiles transmitted by the exit aperture versus the ratio of the orbit radius r of the scattered projectiles to the aperture radius R.

C. Evaluation and discussion

During the course of the present experiment it was necessary prior to the start of each cross-section measurement, to maximize the beam transmission through the scattering region with no target gas present, which involved tuning the many variable parameters that are used to control the projectile beam. In general, the values of B_S and B_A are adjusted to the lowest values consistent with maximum beam transmission to the detector. The effective magnetic field B_R near the center of the retarding element was determined to be $0.57B_A$. It is often the case that two different runs at the same energy with the same projectile will have different combinations of the various parameters.

In order to summarize the angular discriminations, due to the retarding potential procedure and the effect of the exit aperture size, for the various projectiles and the various gases over the spectrum of projectile energies, the values for $\theta_S(R)$ and $\theta_S(A)$ from Eqs. (6) and (10) (with $r_A = 1.55$ mm) have been calculated for each measurement. The results of these determinations are given in Table I. In most cases more than one measurement was made for a given projectile, target gas, and energy, in which case the angular discrimination values in Table I represent the averages of the various individual values. In a few measurements, a parameter value was not recorded and, as a result, no angular discrimination value is given.

In considering the information presented in Table I it should be realized that the two different effects providing discrimination against small-angle scattering are independent from each other in that each effect would provide discrimination without the existence of the other effect. As a result, one should expect that whichever effect gives the best angular discrimination (smallest angle) for a given measurement, this value should represent an upper limit for the angular discrimination since the other effect, even though it gives a larger angle, will still provide some additional discrimination and improve the overall discrimination. In the cases where the associated

TABLE I. Angular discriminations (in degrees) deduced for the retarding potential procedure (R values) and for the effect due to the exit aperture size (A values). The columns are also labeled according to the target gases and projectile particles.

	Helium		Neon		Argon	
	e^+	e^-	e^+	e^-	e^+	e^-
Energy (eV)	R,A	R,A	R,A	R,A	R,A	R,A
20			25,24	24,9	64,10	24,10
30		22,11	17,25	11,7	17,9	17,10
50	16,18	13,7	19,19	11,8	23,12	14,6
75	16,16	13,4	19,11	9,14		9,7
100	13,8	10,6	21,12	8,6	20,8	10,5
150	12,7	9,5	14,10	7,5	17,8	9,6
200	14,7	12,8	11,7	9,6	13,7	7,6
300	6,6	8,6	12,7	9,6	8,6	6,5
400	7,6	10,6	10,6	7,6	9,7	7,6
500	8,6	5,5	9,6	7,6	9,6	7,6
600	8,6	8,6	11,7	8,6	18,7	8,6
700			10,6		13,7	7,6
800					6	6,5

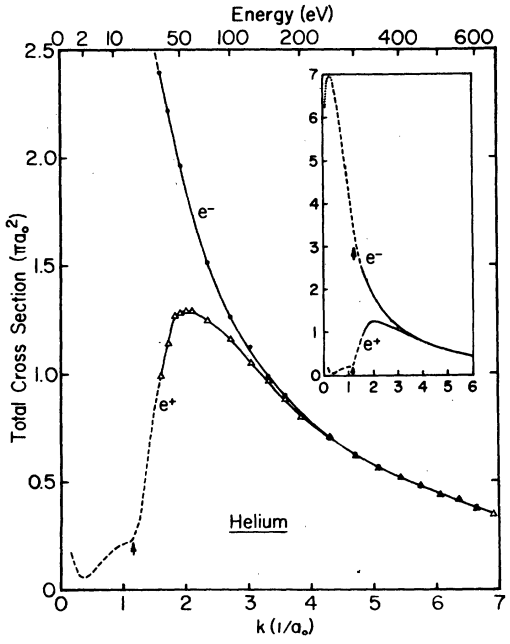

FIG. 3. Total electron- and positron-helium scattering cross sections. The present results for electrons(·) and positrons(△) are shown with a solid line drawn through the respective points. The dashed line at low energies for positrons represents the data of Stein *et al.* (Ref. 12). The dashed portion of the curve for electrons (shown in the inset) is from Kauppila *et al.* (Ref. 4) and the dotted portion at the lowest energies is from Milloy and Crompton (Ref. 3). The lowest-energy inelastic thresholds for each projectile are indicated by arrows and correspond to positronium formation at 17.8 eV for positrons and atomic excitation at 19.8 eV for electrons.

R and A values in Table I are the same we would expect the overall angular discrimination, due to a combination of these two effects, to be somewhat better than either value separately. In summary, the smaller angle of each pair of R and A values should be a reasonable estimate of an upper limit on the angular discrimination which can be used along with elastic differential cross sections, if available from experiments or theory, to make estimates of the associated errors that may be expected in the present total-cross-section measurements (see Sec. IV).

IV. TOTAL-CROSS-SECTION RESULTS AND DISCUSSION

A. Positron- and electron-helium measurements

The present measurements of total cross sections for positrons and electrons colliding with helium atoms are shown in Fig. 3, and are compared with various recent theoretical calculations[21,35-40] and with several prior experimental results[5,20,41-44] in Table II. Only the more recent electron measurements are included in Table II (and Tables III and IV) in order to simplify the overall comparisons between the electron and positron experimental and theoretical results. The most striking feature of the present results is the merging (to within 2%) of the positron and electron total scattering cross sections at 200 eV. This observed merging is of particular significance because the positron and electron measurements (of which preliminary results were presented elsewhere[45]) represent the first set of results at these intermediate energies where both projectiles have been used in the same experimental system with the same experimental approach. This approach is advantageous in that most systematic errors in the determination of target-gas number densities and projectile beam path lengths through the gas scattering region tend to equally affect the positron and electron measurements. As a result, the comparisons of the relative positron and electron measurements are more meaningful than the separate absolute cross-section values.

One known source of error that could have influenced the observed merging of the electron and positron total scattering cross sections is the inability of this experiment to fully discriminate against small-angle forward elastic scattering. It is evident from some of the current theories (for example, see Fig. 1 in Ref. 21 and compare Tables I and VI in Ref. 35) that the elastic scattering of electrons by helium at intermediate energies is more pronounced at the smallest scattering angles than it is for positrons, while

TABLE II. Total cross sections for positron- (electron-)helium scattering (in units of πa_0^2). The positron values are shown without parentheses while the electron values are enclosed in parentheses. The BB values, enclosed by dashes, apply to both positrons and electrons. Values followed by "*i*" are interpolated values. Experimental values for e^--He of Kennerly and Bonham (Ref. 5) are (2.68) for 30 eV and (1.91) for 50 eV.

Energy (eV)	This experiment	Theoretical values DWSBA[a]	OM[b]	EBS[c]	BB[d]	BG+DW[e]	MG[f]	Experimental values B[g]	G[h]	J[i]	BL[j]	D[k]
30	(2.66)							0.78	0.80		(2.64)	(2.80)
50	1.27(1.97)						0.93	1.26	1.20	1.22*i*	(1.93)	(2.06)
75	1.24(1.51)									1.26*i*	(1.45)	(1.56*i*)
100	1.16(1.26)	1.20(1.74)	1.26(1.96)	0.723(1.29)			1.13	1.04	1.07	1.14*i*	(1.24)	(1.30)
125	1.05(1.12)								1.00	0.97*i*	(1.08*i*)	
150	0.967(0.987)				-1.18-		0.903		0.92	0.94*i*	(0.964)	(1.00)
175	0.880(0.897)								0.80	0.80*i*	(0.880*i*)	
200	0.796(0.812)	0.845(1.02)	0.853(1.07)	0.726(0.878)	-0.951-	0.799(0.907)	0.825	0.82	0.73	0.79*i*	(0.805)	(0.836)
250	0.705(0.702)				-0.800-				0.61	0.69*i*	(0.694)	
300	0.614(0.621)	0.650(0.738)	0.653(0.758)	0.592(0.659)	-0.693-	0.618(0.668)	0.636	0.65	0.54		(0.614)	(0.629)
400	0.516(0.515)	0.531(0.583)	0.532(0.592)	0.493(0.532)	-0.551-	0.506(0.535)	0.519	0.53	0.44		(0.500)	(0.511)
500	0.437(0.434)	0.450(0.485)	0.452(0.490)	0.423(0.446)	-0.459-	0.430(0.449)	0.440	0.42	0.44		(0.420)	(0.432)
600	0.371(0.381)				-0.396-		0.350	0.41	0.35		(0.372)	
700		0.348(0.367)	(0.369)	0.331(0.341)	-0.349-	0.333(0.342)	0.311	0.33	0.30		(0.331)	(0.330)
1000		0.262(0.272)			-0.259-	0.251(0.255)	0.234	0.24	0.10			(0.243)
2000		0.148(0.151)				0.142(0.143)						(0.140)
3000		0.105(0.106)				0.101(0.101)						(0.098)

[a] DWSBA (distorted-wave second Born approximation); Dewangen and Walters, Ref. 21.
[b] OM (optical model); Byron and Joachin, Ref. 35.
[c] EBS (eikonal-Born series); Byron, Ref. 36.
[d] BB (Bethe-Born); Inokuti *et al.*, Refs. 37 and 38.
[e] BG+DW (Bethe theory with gamma term for inelastic cross section; DWSBA for elastic cross section); Inokuti *et al.*, Ref. 39; Dewangen and Walters, Ref. 21.
[f] MG (modified Glauber); Gien, Ref. 40.
[g] B: Brenton *et al.*, Ref. 20.
[h] G: Griffith *et al.*, Ref. 41.
[i] J: Jaduszliwer *et al.*, Ref. 42.
[j] BL: Blaauw *et al.*, Ref. 43.
[k] D: de Heer and Jansen, Ref. 44 (semiempirical).

TABLE III. Total cross sections for positron- (electron-)neon scattering (in units of πa_0^2). Other explanatory information is the same as for Table II. Experimental value for e^--Ne of Salop and Nakano (Ref. 51) is (4.13) for 20 eV.

Energy (eV)	This experiment	Theoretical values DWSBA[a]	OM[b]	BB[c]	BG+DW[d]	Experimental values B[e]	C[f]	T[g]	D[h]	W[i]
20	1.62(4.19)					1.52	1.42*i*		(3.92)	
30	2.01(4.23)					1.76*i*	1.86*i*	1.85	(3.84)	(4.28)
50	2.25(4.05)					2.20		2.02	(4.03)	(4.08)
75	2.26(3.72)						2.5	2.05*i*	(3.95*i*)	(3.78)
100	2.17(3.37)		2.68(4.52)			2.05	2.25	2.08	(3.71)	(3.44)
150	2.02(2.87)			-7.07-			1.95	1.86	(2.94)	(2.96)
200	1.90(2.54)	2.20(3.11)	2.15(3.07)	-5.52-	2.15(2.88)	1.84	1.70	1.79	(2.54)	(2.64)
300	1.60(2.03)	1.86(2.43)	1.81(2.40)	-3.92-	1.80(2.28)		1.16		(2.11)	(2.12)
400	1.39(1.74)	1.61(2.02)	1.58(2.00)	-3.05-	1.55(1.91)	1.42	1.05		(1.75)	(1.80)
500	1.23(1.52)	1.42(1.74)	1.40(1.73)	-2.49-	1.37(1.65)		0.68		(1.52)	(1.57)
600	1.10(1.36)			-2.12-		1.15	0.63			(1.38)
700	1.04(1.24*i*)	1.17(1.39)	- (1.40)	-1.85-	1.12(1.32)	1.02*i*	0.55		(1.24)	(1.26)
1000		0.93(1.08)		-1.34-	0.90(1.03)	0.75			(0.94)	
2000		0.58(0.64)			0.55(0.61)				(0.57)	
3000		0.42(0.46)			0.40(0.44)				(0.41)	

[a] DWSBA (distorted-wave second Born approximation); Dewangen and Walters, Ref. 21.
[b] OM (optical model); Byron and Joachain, Ref. 35.
[c] BB (Bethe-Born); Inokuti and McDowell, Ref. 38; Saxon, Ref. 46.
[d] BG+DW (Bethe theory with gamma term for inelastic cross section; DWSBA for elastic cross section); Inokuti *et al.*, Ref. 39 and Saxon, Ref. 46; Dewangen and Walters, Ref. 21.
[e] B: Brenton *et al.*, Ref. 47.
[f] C: Coleman *et al.*, Ref. 48.
[g] T: Tsai *et al.*, Ref. 31.
[h] D: de Heer *et al.* (semiempirical), Ref. 49.
[i] W: Wagenaar and de Heer, Ref. 50.

at the larger angles the scattering becomes quite similar. The more pronounced differences at small angles for these two projectiles is attributed[35] to the effect of the polarization potential and how it adds to (for electron impact) and subtracts from (for positron impact) the effect of the static potential for the respective projectile particles. In order to estimate the possible errors in the present total-cross-section measurements due to this possible lack of discrimination against small-angle forward elastic scattering it is necessary to consider the angular discrimination of the experiment (see Sec. III), the elastic differential scattering cross sections, and the fraction of the total cross section that is attributable to elastic scattering. In the case of the elastic differential cross sections at these intermediate energies, experimental results are available only for electron scattering and are in very good agreement above 200 eV with the calculations of Byron and Joachain,[35] who use an eikonal-Born-series method within the framework of the optical-model formalism [hereafter referred to as the "optical model" (OM)], and the distorted-wave second Born approximation (DWSBA) calculation of Dewangen and Walters.[21] The optical-model results[35] (which are generally in very good agreement with the DWSBA results[21]) are used for the elastic differential cross sections and for the ratios of the elastic scattering cross sections to the total cross sections, while the smaller discrimination angle of each pair of the R and A values in Table I are used in making estimates of the errors that may arise in the present measurements due to a lack of complete discrimination against small-angle forward elastic scattering. In the range of energies from 100 to 500 eV (where this experiment and the theory[35] overlap) these estimated errors average 2% for electrons and 1% for positrons, implying that the actual total cross sections may be larger by these amounts. As a result, this lack of discrimination could have made the measured electron and positron total scattering cross sections 1% closer together than the actual cross-section values for energies at and above 100 eV.

Since the incomplete small-angle discrimination in the present experiment should have little overall effect on the observed merging of the positron and electron cross sections, it is of interest to compare these results with the DWSBA calculation of Dewangen and Walters[21] which extend up to 3000 eV and indicate a merging of the positron and electron cross sections to within 2% at 2000 eV and 1% at 3000 eV. At 200 eV the DWSBA electron total cross section is 20% larger than

TABLE IV. Total cross sections for positron- (electron-)argon scattering (in units of πa_0^2). Other explanatory information is the same as for Table II. Experimental values for e^--Ar of Golden and Bandel (Ref. 54) are (21.7i) for 15 eV and (17.1i) for 20 eV.

Energy (eV)	This experiment	Theoretical values				Experimental values			
		OM I[a]	OM II[b]	BG+OM I[c]	B[d]	G[e]	T[f]	D[g]	W[h]
15	6.65(24.5)								(25.8)
20	7.27(19.7)					7.9		(24.9)	(23.0)
30	8.19(14.7)					8.3		(18.6)	(15.8)
50	8.34(11.3)					8.95	8.32	(12.7)	(11.6)
75	7.69(9.52)						7.46	(10.6i)	(10.1)
100	7.14(8.72)	7.10(10.0)	7.26(10.6)	(6.07)		7.5	6.96	(9.41)	(9.24)
150	6.10(7.21)					6.2	6.13	(7.88)	(7.84)
200	5.55(6.38)	5.73(7.19)	5.63(7.32)	(6.00)	5.69	4.85	5.33	(6.80)	(6.66)
300	4.53(5.23)	4.87(5.83)	4.74(5.79)	(5.12)		4.1	4.41	(5.35)	(5.45)
400	3.92(4.37)	4.27(4.96)	4.14(4.90)	4.05(4.46)	4.52	2.9		(4.54)	(4.65)
500	3.38(3.74)	3.82(4.36)	3.69(4.27)	(3.96)	3.56	2.8		(3.98)	(4.08)
600	2.96(3.33)				2.99	1.9			(3.65)
700	2.64(3.03)	3.16(3.50)		(3.27)	2.48				(3.31)
800	2.46(2.86)	2.91(3.21)	2.85(3.18)	(3.01)	2.40				
1000		2.52(2.75)	(2.75)	(2.62)	2.34			(2.53)	

[a] OM I (optical-model method I); Joachain *et al.*, Ref. 52.
[b] OM II (optical-model method II); Joachain *et al.*, Ref. 52.
[c] BG+OMI (Bethe theory with gamma term for inelastic cross section; OMI for elastic cross section); Inokuti *et al.*; Ref. 39, and Joachain *et al.*, Ref. 52.
[d] B: Brenton *et al.*, Ref. 47.
[e] G: Griffith *et al.*, Ref. 53.
[f] T: Tsai *et al.*, Ref. 31.
[g] D: de Heer *et al.*, Ref. 49 (semiempirical).
[h] W: Wagenaar and de Heer, Ref. 50.

the positron cross section. The results of the optical-model calculation by Byron and Joachain,[35] extending up to 500 eV for positrons and 700 eV for electrons, are in very good agreement with the DWSBA, while the "eikonal-Born-series" (EBS) calculation of Byron[36] gives cross sections which appear to be merging at a somewhat lower energy than the DWSBA, with the electron values being only 3% larger than the positron values at 700 eV. In any case, the present experimental results are observed to merge at a lower energy than predicted by any of these current theories.

A comparison of the absolute values of the experimentally determined total cross sections in Table II shows that the present electron scattering measurements are in very good agreement (within 5%) at all energies of overlap with the recent measurements of Kennerly and Bonham,[5] and Blaauw *et al.*,[43] and the semiempirical total cross sections deduced by de Heer and Jansen.[44] It should be noted that the angular discrimination of the experiment of Blaauw *et al.*[43] is less than 1° which would result in less than a 0.1% error in their cross-section values due to this effect in the energy range from 100 to 700 eV. Since the present results average 2% higher than Blaauw *et al.*[43] in this same energy range, the actual discrepancy may be 4% (with the present values being higher) if allowance is made for the estimated angular discrimination corrections. The present positron total scattering cross-section measurements are in fair to good agreement (within 15%) with the measurements of Brenton *et al.*,[20] Griffith *et al.*,[41] and Jaduszliwer *et al.*[42] In comparing the present total-cross-section values with the theoretical results, one finds that the DWSBA[21] and optical-model[35] results are higher for both positron and electron scattering, with the theoretical results approaching experiment at the highest energies. In general, the positron values are in closer agreement (differing by 3% at 500 eV) than the electron values (differing by 12% at 500 eV). The EBS[36] results bracket the experimental results in that the theoretical electron values are generally higher (by 3% at 500 eV) than the experimental values while the theoretical positron values are lower (by 3% at 500 eV). A "Bethe-Born" total-cross-section calculation (in which no distinction is made between positron or electron projectiles) by Inokuti *et al.*,[37,38] where the Bethe theory was used to determine the inelastic cross sections[37] and the first Born approximation to determine the elastic cross sections,[38] gives results that are somewhat higher than both the positron and electron experimental results, but lie between the positron and electron results from

the DWSBA and optical-model calculations. In surveying the various theoretical results it has been found that by adding the inelastic cross sections that can be calculated by using the Bethe theory with an additional "gamma" term[39] (which relates to the number of electrons in the target atom) and the elastic scattering cross sections resulting from the DWSBA theory,[21] one obtains total cross sections (designated by BG+DW in Table II) that agree to within 2% with the present positron results at and above 200 eV and differ by less than 10% for electron scattering. It is also interesting that the BG+DW positron and electron values appear to be merging at a somewhat lower energy than the other calculations presented here. A recent "modified Glauber" calculation by Gien[40] for positron total scattering gives results which agree quite well with the present results for energies above 200 eV.

B. Positron- and electron-neon measurements

The present total-cross-section measurements for positrons and electrons colliding with neon atoms are shown in Fig. 4, and are compared with several theoretical calculations[21,35,38,39,46] and prior experimental results[31,47-51] in Table III. The measured total-cross-section curves displayed in Fig. 4 are seen to be slowly approaching each other as the energy increases with the electron results being about 20% higher than the positron results at 700 eV. Estimates of the possible errors due to incomplete discrimination against small-angle forward scattering have been made using the same procedure that was used for scattering from helium, with the optical-model results of Byron and Joachain[35] being used for the differential elastic scattering cross sections and for obtaining the fraction of the total cross section that is attributable to elastic scattering. These estimates indicate that the present measurements may be an average of 4% too low for positrons and 5% too low for electrons in the energy range from 100 to 500 eV. As a result, the comparison of the present positron and electron relative total-cross-section results should be little affected by this consideration. In comparing the gradual approach of the measured cross sections with the DWSBA calculation of Dewangen and Walters[21] (which agrees well with the optical-model calculation of Byron and Joachain[35] in the region of overlap) one finds a quite similar behavior where the theoretical results for electron scattering are about 20% higher than the positron values at 700 eV and this difference decreases to about 10% at 3000 eV.

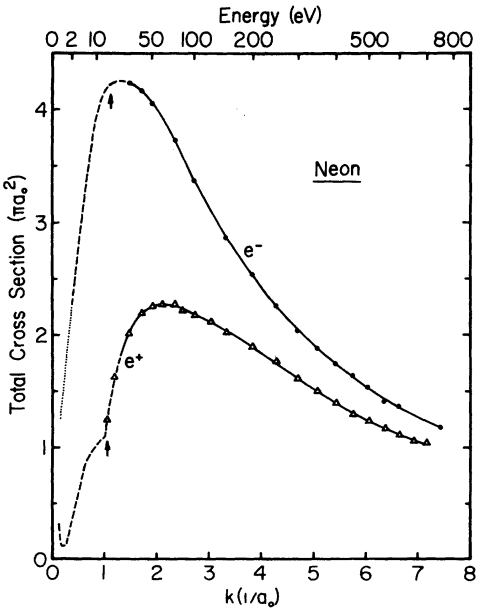

FIG. 4. Total electron- and positron-neon scattering cross sections. The present results are indicated by (·) for electrons and (△) for positrons with solid lines drawn through the respective points. The dashed lines at low energies for positrons and electrons represent the results of Stein *et al.* (Ref. 12), while the dotted line at the lowest energies for electrons is from Salop and Nakano (Ref. 51). The arrows refer to the lowest-energy inelastic thresholds for positrons (14.8 eV for positronium formation) and electrons (16.6 eV for atomic excitation).

The present absolute e^--Ne total-cross-section values are slightly lower (an average of 3% in the range from 100 to 500 eV) than Wagenaar and de Heer,[50] in very good agreement at 20 eV with Salop and Nakano,[51] and in good agreement with the semiempirical results obtained by de Heer *et al.*[49] The angular discrimination of the experiment of Wagenaar and de Heer[50] (less than 1°) would result in less than a 0.2% error in their cross-section values from 100 to 500 eV, which would indicate that the discrepancy between the present results and Wagenaar and de Heer would be 2% (with the present results being higher) if allowance is made for the estimated angular discrimination corrections. For positron scattering the present measurements are in good agreement with Brenton *et al.*,[47] where the present results are an average of a few percent higher. The measurements of Coleman *et al.*[48] are in fair agreement with the present results up to 200 eV, but decrease rapidly at higher energies, which is most likely due to their inability to discriminate against all of the inelastically scattered positrons and positrons elastically scattered at small angles in the forward direction. The total-cross-section values measured by Tsai *et al.*[31] are consistently about 8% lower than the present measurements.

The theoretical results from the DWSBA[21] and optical-model[35] calculations are higher than the present measurements by nearly the same amount for positron and electron scattering, ranging from 20 to 25% higher at 100 eV to about 10% higher at 700 eV. For $e^{\pm}$ scattering by neon, the Bethe-Born calculations,[38,46] where the Bethe theory is used to determine the inelastic scattering cross section and the first Born approximation for the elastic cross section, do not seem to give very good results. Meanwhile, it is interesting that when inelastic cross sections are calculated by using the Bethe theory with the additional gamma term,[39,46] and these inelastic cross sections are added to the elastic cross sections obtained from the DWSBA[21] theory, one gets total-cross-section values that are in better agreement with the experimental results than either the DWSBA or optical-model calculations.

C. Positron- and electron-argon measurements

The present results with argon atoms as the target particles are shown in Fig. 5 and compared with theory[39,52] and other experimental results[31,47,49,50,53,54] in Table IV. From Fig. 5 it is seen that the electron and positron total-cross-section curves are only slowly approaching each other at the highest measured energies. The optical-model calculations of Joachain *et al.*[52] indicate a rather similar gradual approach of the electron and positron cross sections. Using the results of "method II" of these calculations[52] along with the deduced angular discriminations given in Table I, it is estimated that the present total-cross-section measurements for electron scattering may be an average of 9% too low in the energy range from 100 to 800 eV and 10% too low for positrons at 400 eV (the only energy for which theoretical results were readily available).

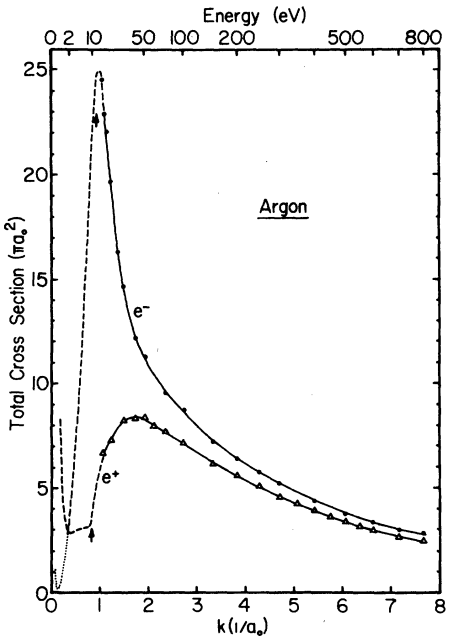

FIG. 5. Total electron- and positron-argon scattering cross sections. The present results are indicated by (·) for electrons and (△) for positrons. The dashed lines for electrons and positrons represent the measurements of Kauppila *et al.* (Ref. 17), while the dotted line at the lowest energies for electrons is taken from Golden and Bandel (Ref. 54). The arrows indicate the lowest-energy inelastic thresholds for positrons (9.0 eV for positronium formation) and electrons (11.5 eV for atomic excitation).

A comparison of the present e^--Ar results for energies above 100 eV with Wagenaar and de Heer[50] (whose angular discrimination of less than 1° would cause an error in their cross-section measurements of less than 0.4%) finds the present results to average 7% lower. If an allowance is made for the estimated corrections due to incomplete angular discrimination in these experiments, the present results would average about 2% higher. Below 100 eV Wagenaar and de Heer also average 7% higher. The semi-empirical electron results of de Heer *et al.*[49] average 6% (and 16%) higher than the present results above 100 eV (and below 100 eV). The electron measurements of Golden and Bandel[54] are 10–15% lower than the present results at 15 and 20 eV. The present positron measurements are an average of 2% lower than the results of Brenton *et al.*[47] and 2% higher than the measurements of Tsai *et al.*,[31] while the measurements of Griffith *et al.*[53] range from about 5% higher at the lower energies to considerably lower (> 20%) at the highest energies of comparison.

Comparing the present total-cross-section measurements with the optical-model calculations [methods I (OMI) and II (OMII)] of Joachain *et al.*[52] it is found, if an allowance is made for the estimated potential small-angle forward elastic scattering errors, that there is agreement to within 10% at all energies. It should be pointed out, however, that for each projectile, the present results are diverging slightly from these theoretical results at the highest energies of overlap. The theoretical results, labeled BG+OMI in Table IV, have been obtained by using the Bethe theory with the additional gamma term[39] for the inelastic cross section and the optical-model (method I)[52] results for the elastic scattering cross section. This hybrid theory gives results for electrons which are quite low for energies up to 200 eV but seem to be closely approaching the present results, if corrected, at the highest energies.

D. General discussion

The most obvious features that are apparent from Figs. 2, 3, and 4 are that the electron total scattering cross sections are always larger than the positron curves, except when the Ramsauer-Townsend effect results in an abnormally low electron cross section, as for argon scattering. It is interesting to observe that the electron curves for these three gases reach their maximum values either below or near the lowest inelastic threshold energies (corresponding to atomic excitation) which indicates that elastic scattering is the predominant scattering process in the vicinity of these peaks. Meanwhile, the positron curves reach their peaks at higher energies, which are above the onset of inelastic scattering processes (where positronium formation gives the lowest-energy inelastic thresholds and these peaks appear to be associated with inelastic processes. It would be very interesting to study the respective roles of elastic and inelastic scattering of positrons in the energy range extending upward from the inelastic thresholds. Prior work[12,17] indicates that for neon and argon an appreciable contribution to inelastic scattering may be due to positronium formation. The DWSBA calculations of Dewangen and Walters[21] predict that the ratio of Q(elastic)/Q(tot) for positrons (electrons) scattered by helium varies from 0.15 for e^+ (0.44 for e^-) at 100 eV to 0.14 (0.15) at 3000 eV, which implies that at intermediate energies, inelastic processes play a more important role in the total scattering of positrons by helium than for electrons. Using results from the DWSBA theory[21] for neon one gets ratios for Q(elastic)/Q(tot) ranging from 0.35 for e^+ (0.56 for e^-) at 200 eV to 0.49 (0.53) at 3000 eV.

Comparisons of the present measurements with other experiments reveals a remarkable consistency with the electron total-cross-section measurements made at the FOM Institute.[43,50] The present values, if corrected for the estimated angular discriminations against small-angle forward elastic scattering, average 4, 2, and 2% higher than the FOM results for helium, neon, and argon, respectively, for energies above 100 eV. If the projected "corrections" to the present values are reliable (they depend on the estimated angular discriminations and also the theories used to obtain the differential elastic scattering information), it would appear that there is a systematic discrepancy of a few percent between these two experiments, which would be well within the estimated systematic errors of each experiment. For positron scattering from helium, neon, and argon the present results are in generally good agreement with the results from the experimental groups at Swansea,[20,47] London,[41,48,53] and Toronto,[31,42] except at the higher energies where the London results fall off more rapidly due to deterioration of their discrimination against inelastically scattered particles and elastically scattered particles at small angles in the forward direction.

In comparing the present measurements with several of the applicable theories it is interesting to note that the Bethe theory with the additional gamma term,[39,46] which relates to the number of electrons in the target, seems to give better results for the inelastic cross sections for He, Ne, and Ar than the other theories. This observation requires that the elastic cross sections determined from the DWSBA theory[21] (for helium and neon) and the optical-model (method I) theory[52] (for argon) are reasonably accurate, which seems to be the case when they are compared with experimental measurements of electron differential elastic scattering cross sections (refer to the respective theoretical papers). In order to provide more stringent tests of various theories it will be of considerable interest to study differential elastic scattering of positrons by atoms and molecules.

V. ERROR ANALYSIS

In addition to the problem of discrimination against projectiles that experience small-angle forward elastic scattering (which always results in measured cross sections that are too low), measurements of total scattering cross sections are also subject to a variety of other potential systematic errors, as well as statistical counting errors. From Eq. (2) we find that the measurements of Q_T are dependent on the reliability of the measurements of the target-gas number density n, the beam path length L through the scattering region, and measurements of the transmitted projectile beam currents with and without gas in the scattering region I and I_0. In this experiment the statistical errors associated with counting the projectile beam particles are typically 2% for positrons and 1% for electrons.

A. Target-gas number density

The target-gas number density is determined from the expressions[4]

$$n = P_s/k_B T_s \tag{11}$$

and

$$P_s = P_m (T_s/T_m)^{1/2}, \tag{12}$$

where P_s is the pressure in the scattering region,

P_m is the pressure at the capacitance manometer, T_s and T_m are the measured temperatures of the scattering region and manometer, and k_B is the Boltzmann's constant. It has been observed that the pressure at the detector end (the gas-inlet end) of the scattering region is 10% higher than at the beam-source end. The pressure used in Eq. (11) is the average of the pressures at the two ends and has an estimated uncertainty of 2% due to this effect. During the total-cross-section measurements the target gas is repeatedly cycled in and out of the scattering region with a full cycle typically taking 2 min. During the gas-in portion of the cycle the pressure is continuously monitored to account for small variations and it is estimated that the uncertainty in the average pressure during each cycle due to this effect is 1%. The capacitance manometer,[55] which has not been independently calibrated, has a manufacturer's quoted system error of less than 1% for measured pressures greater than 10^{-4} Torr (as used in this experiment). The reliability of a similar capacitance manometer has been examined by Loriot and Moran[56] for measured pressures less than 2×10^{-4} Torr, and an estimated accuracy of 2% plus 4×10^{-7} Torr, in addition to readout limitations, was assigned to their device. Van Zyl *et al.*[57] have calibrated a different model capacitance manometer from the same manufacturer at pressures above 5×10^{-2} Torr and have found it to be accurate to within 2.5%. In the present experiment it is assumed that the readings made with the capacitance manometer are accurate to within 3%. The use of Eq. (12) to correct for thermal transpiration effects between the thermally controlled capacitance manometer head and the scattering region has previously been discussed[4] and its use is consistent with the findings of Loriot and Moran.[56] An uncertainty of 1% is assigned to account for the use of Eq. (12) and the uncertainties in the measurements of T_s and T_m (where T_s is continuously recorded and typically between 295 and 300 K, while T_m is maintained at 322 K with the accuracy of each measurement being ±1 K). Another potential source of error is that of gas impurities. In the present experiment research grade gases (99.999% purity) are used with no independent tests being made of the gas purity in the scattering region. An important part of every separate cross-section-measurement run at a given energy was to measure the total cross sections for a widely varying range of target-gas number densities to check that the measured cross sections for every run are independent of the target-gas number density. Examples of the pressure independence of the measured cross sections for typical runs are shown in Fig. 6. It is seen from Fig. 6 that in several cases the ratios of I/I_0 range from less than 0.2 to more than 0.8, which would correspond to a pressure (number density) variation of more than a factor of 7. For the measurements resulting in the smallest cross-section values (namely, for helium at energies above 200 eV) values of I/I_0 below 0.5 could not be obtained out of considerations for the highest pressures at which the channeltron detector can be safely operated.[12] The independence of the measured cross sections on the target-gas pressure is an indication that several potential systematic errors should be negligible, unless some remarkable coincidences occur where two errors cancel in such a way as to give this pressure independence. It seems unlikely that target gas entering the source and detector regions[4] could be affecting the emission or detection of the projectile beam particles. It also seems unlikely that multiple scattering of the projectile beam particles could be affecting these measurements. The pressure independence of the measured cross sections is also an indication that residual background gases should not be affecting the target-gas purity to any noticeable extent.

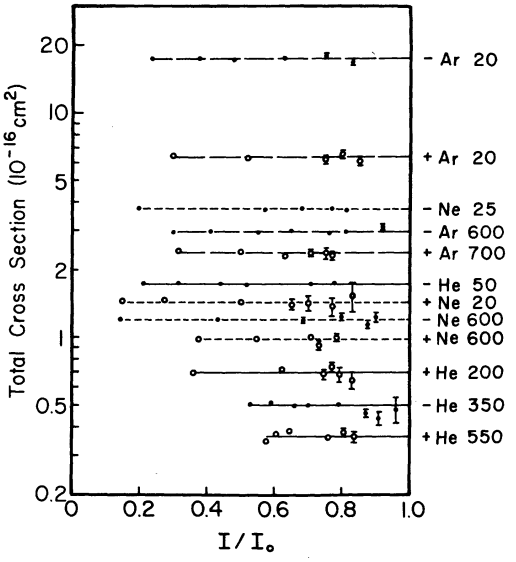

FIG. 6. Measured total cross sections versus attenuation ratio I/I_0 for various projectile-target combinations. The projectiles are labeled (+) for positrons and (–) for electrons. The numbers following the target-gas symbols are the projectile energies in eV. Statistical uncertainties of one standard deviation in the measured cross sections are represented by the error bars except where they are encompassed by the sizes of the dots or circles.

B. Beam path length

The beam path length through the gas scattering region is dependent on the measured length of the

scattering region, the effect of the pressure drops at the differentially pumped entrance and exit apertures, and the effect of spiralling in the axial magnetic field. The measured length of the scattering region is 109 cm with an uncertainty of ±0.5%. The pressure drops at the entrance (diameter, 3.2 mm) and the exit (diameter, 4.8 mm) apertures should have less than a 0.5% effect on the path length. No evidence of a beam path length increase due to spiralling has ever been observed with this transmission experiment despite several attempts to create such an effect by varying (1) the magnetic field in the scattering region and (2) using various beam-optics focusing conditions. An earlier estimate[4] of 1% is assigned as a reasonable upper limit for the error in path length due to spiralling.

C. Projectile beam currents

The positron- and electron-beam currents were both detected with a channeltron electron multiplier (in a counting mode). The maximum count rates used were 5000/sec for positrons and 20 000/sec for electrons, which means that space-charge effects were negligible. During the course of the measurements the positron currents differed by more than a factor of 10 between different runs at the same energy, while electron currents differed by more than a factor of 3. In both cases, there was no evidence of any nonlinearities in the counting electronics. For the transmitted positron and electron beams, when target gas was present, the independence of the measured cross sections versus I/I_0 in Fig. 6, where the transmitted beam varied from less than 20% to more than 80% of I, is a further indication of the linearity of the beam-detection system. One difference between the electron and positron beams is that the primary electron-beam current was constant during the measurements, while the primary positron-beam current was always decreasing due to the 20-min half-life of the ^{11}C positron source. The length of time for cycling the gas in and out of the scattering region was chosen to be only 2 min (for a complete cycle from the start of one gas-out reading, through a gas-in reading, to the start of another gas-out reading) in order that the exponential decay of the beam would have less than a 0.5% effect on the cross-section measurements. Corrections to the cross sections due to noise counts have been treated in a manner as discussed by Stein *et al.*[12] The noise arises principally from beam particles having energies in the "high-energy tails" of the beam energy distributions (see Stein *et al.*[33,58] for examples of these distributions made at low energies when no entrance and exit apertures to the solenoid are present). For the electron measurements, the uncertainties in the measured cross sections due to this noise component are negligible, while for positrons this uncertainty is estimated to be largest (a maximum of 1%) for the lowest signal-to-noise ratios that were used. The uncertainties in assigning energies to the projectile beams are estimated to be about ±1.0-eV above 100 eV and less than ±0.5 eV below 100 eV. These energy uncertainties would result in total-cross-section uncertainties of less than 0.5%, except possibly for e^--Ar scattering below 30 eV where it could be a bit larger due to the rapidly changing cross-section values versus energy.

A potential source of error is related to the usual operating procedure[4,12] of applying a voltage to the retarding element preceding the channeltron so that it passes only 80% of the total primary beam I_t when no target gas is present. Let us define $I_c = 0.8 I_t$. This means that 20% of the beam current is stopped at the retarding element, which we define as I_s $(=0.2 I_t)$. If most of I_s represents projectiles merely having more transverse motion (as opposed to having inherently lower energy which some of these projectiles will have) they could be scattered by gas atoms into a "more-axial" direction and then pass through the retarding potential "hill" and be detected only after they are scattered. This would have the effect of decreasing the measured cross sections. It is determined that the maximum errors due to this effect are 0.5%, 1%, and 2% for $e^{\pm}$ scattering from helium, neon, and argon, respectively.

Another potential systematic error that could affect transmission experiments using an axial magnetic field to confine the projectile beam has been discussed by Golden.[59] A loss of sensitivity to scattering can result if projectile beam particles scattered at angles near 90° do not hit any walls and keep spiralling in the axial field until they again scatter from another atom. There is then a chance that this "doubly scattered" projectile particle may again join the unscattered beam and be detected. In the present experiment this potential source of error is negligible.

D. Summary of experimental errors

The estimated experimental errors in the present measurements (obtained by taking the square root of the sum of the squares of each individual error component, except for the potential small-angle scattering errors) are summarized in Table V for the various projectile-target combinations. The maximum errors (obtained by addition of each individual error component,

TABLE V. Estimated experimental and maximum percentage errors for absolute total-cross-section measurements and the $e^{\pm}$ comparison measurements. The maximum error values are enclosed in parentheses. These estimates do not include the potential errors due to incomplete discrimination against small-angle forward elastic scattering, which has been discussed separately.

Projectile-target system	Absolute measurements	$e^{\pm}$ Comparison measurements
e^+-He	5(14)	3(6)
e^+-Ne	5(14)	3(6)
e^+-Ar	5(15)	3(7)
e^--He	5(11)	2(3)
e^--Ne	5(12)	2(4)
e^--Ar	5(13)	3(5)

except for the potential small-angle scattering errors) are also given in Table V. It is to be noted that separate error values are listed for the absolute total-cross-section measurements, and the positron and electron comparison measurements. The errors for the comparison measurements are appreciably smaller because only the error components associated with the different projectile beam characteristics (statistical, exponential decay, noise, energy, retarding effects, and spiralling effects) will contribute to these "comparison" errors. The other error components will affect the positron and electron measurements in the same way and have no effect on the comparison measurements. The small-angle scattering errors, discussed elsewhere, can affect both the absolute and comparison measurements.

VI. TESTS OF THE SUM RULE

Next we consider the sum rule for positrons and electrons colliding with helium, neon, and argon. We use the sum rule in the form of Eq. (1) in that we assume the projectiles and the target atoms do not form bound states. For electron cases, it is well known that electrons do not bind to ground-state helium, neon, and argon atoms. The absence of a bound state between positrons and some noble gases has been discussed by Golden and Epstein[60] and by Schrader.[61] To evaluate the integral on the right-hand side of Eq. (1) we have fitted our measured (uncorrected) cross sections for low energies[4,12,17] and intermediate energies (present paper) to various analytic functions by dividing the energy region from 0 to ∞ into different segments in order to get better fits. The contribution to the integral from different momentum ranges are summarized in Table VI. Except for the lowest- and highest-

TABLE VI. Contributions to $(1/2\pi)\int_0^\infty Q_t(k)dk$ from different ranges of k ($k_1 \leq k \leq k_2$) for $e^{\pm}$-He, $e^{\pm}$-Ne, and $e^{\pm}$-Ar scattering.

System	k_1	k_2	Contribution
e^--He	0	0.47	0.4879
	0.47	0.9	0.3951
	0.9	1.3	0.2485
	1.3	5.0	0.7423
	5.0	∞	0.6812
		Total	2.5550
e^+-He	0	1.1	0.0290
	1.1	2.0	0.1214
	2.0	3.5	0.2694
	3.5	7.0	0.3128
	7.0	∞	0.5204
		Total	1.2530
e^--Ne	0	0.6	0.1712
	0.6	1.22	0.3848
	1.22	2.71	0.9327
	2.71	4.7	0.8350
	4.7	7.0	0.5874
	7.0	∞	2.1844
		Total	5.0955
e^+-Ne	0	1.0	0.1049
	1.0	2.0	0.3030
	2.0	3.5	0.5153
	3.5	9.0	1.1586
	9.0	∞	1.8004
		Total	3.8822
e^--Ar	0	0.4	0.3635
	0.4	0.7	0.4423
	0.7	1.4	2.3094
	1.4	4.0	3.7885
	4.0	7.0	2.1032
	7.0	∞	5.0524
		Total	14.0593
e^+-Ar	0	0.81	0.9292
	0.81	2.0	1.3809
	2.0	3.5	1.6772
	3.5	9.0	3.0388
	9.0	∞	6.3402
		Total	13.3663

energy regions the total cross sections are fitted, in a straightforward manner, to various polynomials. For the lowest-energy region we employed a five-parameter function,

$$a_1 + a_2 k + a_3 k^2 \ln k + a_4 k^2 + a_5 k^4 ,$$

which is based on a modified effective-range theory[62] taking into account the asymptotic r^{-4} polarization potential. For the numerical fits involving positrons we let all parameters a_1 to a_5 be free. For the electron cases, however, a_1 is kept fixed since electron cross sections are not available (from our group) around thermal

energies. By keeping a_1 fixed at a value of $4a^2$, where a is the scattering length, we force our measured electron cross sections to join the "theoretical" cross sections at zero energy. The values of a are taken as +1.178 (from O'Malley[63]), +0.22 (from Naccache and McDowell[64]), and −1.7 (from O'Malley[62]) for e^--He, e^--Ne, and e^--Ar, respectively. These values are deduced from momentum-transfer cross-section measurements by using the modified effective-range theory. The functional form used in the highest-energy region is

$$\frac{1}{k^2}\left(b_1 + b_2 \ln k^2 + \frac{b_3}{k^2} + \frac{b_4}{k^4}\right).$$

When we fit our measured cross sections to the above formula, b_3 and b_4 are variable parameters but b_1 and b_2 are taken to be the leading coefficients of theoretical Born cross sections, which is equivalent to joining smoothly the measured cross sections to the Born approximation results. The fixed values of b_1 and b_2 are 6.18 and 3.011 for $e^{\pm}$-He scattering[38], 63.29 and 7.7 for Ne scattering[38], and 87.7 and 49.6 for Ar scattering,[31] respectively.

Once the cross sections are fitted to analytic functions, the integral on the right-hand side of Eq. (1) can be readily evaluated. The results together with the various parameters used to test the sum rule are shown in Table VII. For e^--He scattering we adopt a scattering length of 1.178 (from O'Malley[63]) which was deduced from a diffusion cross-section measurement of Crompton *et al.*[65] The direct and exchange amplitudes are taken as 0.796 and 3.943, respectively, from a many parameter Hylleraas wave-function calculation by Ho.[66] These lead to a value of 1.969 for the left-hand side (LHS) of Eq. (1), while the right-hand side (RHS) gives a value of 2.555. It is seen that the sum rule in the form of Eq. (1) does not hold for e^--He scattering. The e^+-He scattering results, on the other hand, are consistent with the sum rule since the experimental cross sections lead to a value of 1.253 for the RHS and the value of the LHS is 1.276 when the scattering length of −0.48 computed by Campeanu and Humberston[15] is used. The present results tend to support previous findings that the sum rule holds for positrons but not for electrons. The inadequacy of the sum rule for electrons has been attributed to singularities in the exchange amplitude (as has been discussed in Sec. I).

The adoption of Campeanu and Humberston's scattering length of −0.48 is not without reservation. It is noted that another elaborate calculation by Page[67] leads to a higher value, −0.44, which differs from −0.48 by about 10%. These calculations were both based on the Kohn variational method. To overcome the difficulty due to inexact target He-wave functions, Campeanu and Humberston used the method of models,[68] while Page used a modified version of Kohn's method. Both calculations relied heavily on the target wave functions, which are inexact. The 10-parameter Hylleraas-type wave function used by Page appears to have a better representation of correlation effects than the 14-parameter wave function used by Campeanu and Humberston since the former included odd powers of r_{12} (the interparticle coordinate between the two target electrons), terms which were omitted in Campeanu and Humberston's wave function. The better representation of correlation effects in Page's wave function also led to a better binding energy, −5.807 Ry, compared with −5.800 Ry obtained by Campeanu and Humberston (the exact energy

TABLE VII. Sum rule tests for $e^{\pm}$-He, $e^{\pm}$-Ne, and $e^{\pm}$-Ar scattering.

System	a	f_B^D	f_B^E	$-a - f_B^D + f_B^E$	$(1/2\pi)\int_0^\infty Q_t(k)dk$
e^--He	+1.178[a]	+0.796[b]	+3.943[b]	1.969	2.555
e^+-He	−0.48[c]	−0.796[b]	0	1.276	1.253
e^--Ne	+0.22[d]	+3.21[e]	+5.321[e]	1.891	5.096
e^+-Ne	−0.614[f]	−3.21[e]	0	3.824	3.882
e^--Ar	−1.7[g]	+9.7[h]	unknown		14.059
e^+-Ar	−3.0 to −4.0[i]	−9.7[h]	0	12.7 to 13.7	13.366

[a] O'Malley, Ref. 63.
[b] Ho, Ref. 66.
[c] Campeanu and Humberston, Ref. 15.
[d] Naccache and McDowell, Ref. 64.
[e] Hutt *et al.*, Ref. 29.
[f] McEachran *et al.*, Ref. 71.
[g] O'Malley, Ref. 62.
[h] Tsai *et al.*, Ref. 31.
[i] Hara and Fraser, Ref. 72.

is[69] −5.807 44 Ry). Campeanu and Humberston's wave function, however, does give the exact polarizability, 1.38, a parameter which is also important in low-energy scattering calculations. The polarizability of Page's wave function has not been determined. If the polarizability of Page's wave function turns out to be exact, it would be more appropriate that the scattering length of −0.44 be adopted. In any case, the 10% difference between these two elaborate calculations indicates a definitive calculation might be obtained only when both correlation and polarization effects are treated correctly.

For e^--Ne scattering we adopt a scattering length of 0.22, a value deduced by Naccache and McDowell[64] by performing a phase-shift analysis on the momentum-transfer cross-section measurements of Robertson.[70] The values of 3.21 for the direct amplitude and 5.321 for the exchange amplitude (as used by Hutt *et al.*[29]) lead to a value of 1.891 for the LHS of the sum rule. The integral on the right-hand side, obtained from the present measurements, gives a value of 5.096. It is concluded that the sum rule fails in e^--Ne scattering. The sum rule for e^+-Ne scattering, on the other hand, seems to hold. If we adopt the scattering length −0.614, obtained from a polarized orbital calculation by McEachran *et al.*,[71] the value of the LHS becomes 3.824 and agrees favorably with the experimentally determined RHS value of 3.882.

The situation for the sum rule tests on $e^\pm$-Ar scattering is less conclusive. To our knowledge, there is no calculation of the exchange amplitude for e^--Ar scattering published in the literature. As a result, no test can be made here. Nevertheless, we show the result of the integral in Table VII for future reference. In addition, by using a scattering length of −1.7 (O'Malley[62]) and a direct amplitude of 9.7 (Tsai *et al.*[31]), we suggest that the sum rule would hold if the exchange amplitude is approximately 22.06. Of course, the condition on the exchange amplitude is dependent on the value of the integral, which may be subject to error due to incomplete discrimination against small-angle forward elastic scattering, and on both the scattering length and the direct amplitude, which may be improved when more elaborate calculations are available. The sum rule for e^+-Ar scattering appears to hold when the scattering length is in the range of −3.0 to −4.0, as deduced by Hara and Fraser[72] from recent annihilation measurements. The LHS of the sum-rule equation probably lies in the range of 12.7 to 13.7. These compare quite well with the RHS value of 13.366 determined from the present measurements. However, a strong conclusion cannot be made at this stage since a polarized orbital calculation by McEachran *et al.*[73] indicates that the scattering length may lie at a lower value of −5.3, and the accuracy for the direct amplitude of −9.7 is not clear.

ACKNOWLEDGMENTS

We would like to express our gratitude to Dr. Mitio Inokuti for providing us with specific details of his Bethe-theory calculations, to Dr. R. W. Wagenaar for sending us a copy of his tabulated results, and to Dr. T. T. Gien and Dr. D. M. Schrader for providing us with their theoretical results prior to publication. We would like to acknowledge the helpful assistance provided by G. Jesion, W. Kaiser, F. Laperriere, M. Scheuerman, and A. Sternad in various aspects of this project. One of us (T.S.S.) acknowledges receipt of an Alfred P. Sloan Foundation Fellowship. This work was supported by the National Science Foundation under Grant No. PHY77-18760.

*Present address: Johns Hopkins University, Applied Physics Laboratory, Laurel, Maryland 20810.

[1]T. C. Griffith and G. R. Heyland, Phys. Rep. 39, 169 (1978).
[2]H. S. W. Massey, Phys. Today 29, 42 (1976).
[3]H. B. Milloy and R. W. Crompton, Phys. Rev. A 15, 1847 (1977).
[4]W. E. Kauppila, T. S. Stein, G. Jesion, M. S. Dababneh, and V. Pol, Rev. Sci. Instrum. 48, 822 (1977).
[5]R. E. Kennerly and R. A. Bonham, Phys. Rev. A 17, 1844 (1978).
[6]A. L. Sinfailam and R. K. Nesbet, Phys. Rev. A 6, 2118 (1972).
[7]J. Callaway, R. W. LaBahn, R. T. Pu, and W. M. Duxler, Phys. Rev. 168, 12 (1968).
[8]T. F. O'Malley, P. G. Burke, and K. A. Berrington, J. Phys. B 12, 953 (1979).
[9]R. K. Nesbet, J. Phys. B 12, L243 (1979).
[10]K. F. Canter, P. G. Coleman, T. C. Griffith, and G. R. Heyland, J. Phys. B 5, L167 (1972).
[11]B. Jaduszliwer and D. A. L. Paul, Can. J. Phys. 51, 1565 (1973).
[12]T. S. Stein, W. E. Kauppila, V. Pol, J. H. Smart, and G. Jesion, Phys. Rev. A 17, 1600 (1978).
[13]J. R. Burciaga, P. G. Coleman, L. M. Diana, and J. D. McNutt, J. Phys. B 10, L569 (1977).
[14]W. G. Wilson, J. Phys. B 11, L629 (1978).
[15]R. I. Campeanu and J. W. Humberston, J. Phys. B 8, L244 (1975); 10, L153 (1977).
[16]J. W. Humberston, J. Phys. B 11, 343 (1978).
[17]W. E. Kauppila, T. S. Stein, and G. Jesion, Phys. Rev. Lett. 36, 580 (1976).

[18]B. H. Bransden and M. R. C. McDowell, Phys. Rep. 30, 207 (1977).
[19]F. W. Byron Jr. and C. J. Joachain, Phys. Rep. 34, 233 (1978).
[20]A. G. Brenton, J. Dutton, F. M. Harris, R. A. Jones, and D. M. Lewis, J. Phys. B 10, 2699 (1977).
[21]D. P. Dewangen and H. R. J. Walters, J. Phys. B 10, 637 (1977).
[22]H. J. Blaauw, F. J. de Heer, R. W. Wagenaar, and D. H. Barends, J. Phys. B 10, L299 (1977).
[23]F. J. de Heer, R. W. Wagenaar, H. J. Blaauw, and A. Tip, J. Phys. B 9, L269 (1976).
[24]B. H. Bransden and M. R. C. McDowell, J. Phys. B 2, 1187 (1969).
[25]E. Gerjuoy and N. A. Krall, Phys. Rev. 119, 705 (1960).
[26]B. H. Bransden and P. K. Hutt, J. Phys. B 8, 603 (1975).
[27]F. J. de Heer, in *Invited Lectures, Review Papers, and Progress Reports of the Ninth International Conference on the Physics of Electronic and Atomic Collisions*, edited by R. Geballe and J. R. Risley (University of Washington Press, Seattle and London, 1976), p. 79.
[28]F. W. Byron Jr., F. J. de Heer, and C. J. Joachain, Phys. Rev. Lett. 35, 1147 (1975).
[29]P. K. Hutt, M. M. Islam, A. Rabheru, and M. R. C. McDowell, J. Phys. B 9, 2447 (1976).
[30]A. Tip, J. Phys. B 10, L11 (1977).
[31]J.-S. Tsai, L. Lebow, and D. A. L. Paul, Can. J. Phys. 54, 1741 (1976).
[32]T. S. Stein, W. E. Kauppila, and L. O. Roellig, Rev. Sci. Instrum. 45, 951 (1974).
[33]T. S. Stein, W. E. Kauppila, and L. O. Roellig, Phys. Lett. 51A, 327 (1975).
[34]J. D. Jackson, *Classical Electrodynamics* (Wiley, New York, 1962).
[35]F. W. Byron Jr. and C. J. Joachain, Phys. Rev. A 15, 128 (1977).
[36]F. W. Byron Jr., Phys. Rev. A 17, 170 (1978).
[37]M. Inokuti, Y.-K. Kim, and R. L. Platzman, Phys. Rev. 164, 55 (1967).
[38]M. Inokuti and M. R. C. McDowell, J. Phys. B 7, 2382 (1974).
[39]M. Inokuti, R. P. Saxon, and J. L. Dehmer, Int. J. Radiat. Phys. Chem. 7, 109 (1975); Y.-K. Kim and M. Inokuti, Phys. Rev. A 3, 665 (1971).
[40]T. T. Gien (private communication).
[41]T. C. Griffith, G. R. Heyland, and T. R. Twomey (unpublished) as reported by T. C. Griffith and G. R. Heyland, Phys. Rep. 39, 169 (1978); T. R. Twomey, T. C. Griffith, and G. R. Heyland, in *Abstracts of the Tenth ICPEAC, Paris, 1977*, edited by M. Barat and J. Reinhardt (Commissariat à L'Energie Atomique, Paris, 1977), p. 808.
[42]B. Jaduszliwer, A. Nakashima, and D. A. L. Paul, Can. J. Phys. 53, 962 (1975).
[43]H. J. Blaauw, F. J. de Heer, R. W. Wagenaar, and D. H. Barends, J. Phys. B 10, L299 (1977) as corrected for incorrect beam path length by R. W. Wagenaar, Ph.D. thesis, FOM Institute Amsterdam, The Netherlands, 1978 (FOMNR 43.948) (unpublished).
[44]F. J. de Heer and R. H. J. Jansen, J. Phys. B 10, 3741 (1977).
[45]W. E. Kauppila, T. S. Stein, G. Jesion, and V. Pol, *Abstracts of the Tenth ICPEAC, Paris, 1977*, edited by M. Barat and J. Reinhardt (Commissariat à L'Energie Atomique, Paris, 1977), p. 802.
[46]R. P. Saxon, Phys. Rev. A 8, 839 (1973).
[47]A. G. Brenton, J. Dutton, and F. M. Harris, J. Phys. B 11, L15 (1978).
[48]P. G. Coleman, T. C. Griffith, G. R. Heyland, and T. R. Twomey, Appl. Phys. 11, 321 (1976).
[49]F. J. de Heer, R. H. J. Jansen, and W. van der Kaay, J. Phys. B 12, 979 (1979).
[50]R. W. Wagenaar and F. J. de Heer, J. Phys. B 13, 3855 (1980).
[51]A. Salop and H. H. Nakano, Phys. Rev. A 2, 127 (1970).
[52]C. J. Joachain, R. Vanderpoorten, K. H. Winters, and F. W. Byron Jr., J. Phys. B 10, 227 (1977).
[53]T. C. Griffith, G. R. Heyland, and T. R. Twomey (unpublished) as reported by T. C. Griffith and G. R. Heyland in Phys. Rep. 39, 169 (1978).
[54]D. E. Golden and H. W. Bandel, Phys. Rev. 149, 58 (1966).
[55]MKS Instruments type 145AH-1 (1 Torr head) with 170 M-9 electronics. The output was read on a digital voltmeter.
[56]G. Loriot and T. Moran, Rev. Sci. Instrum. 46, 140 (1975).
[57]B. Van Zyl, G. E. Chamberlain, G. H. Dunn, and S. Ruthberg, J. Vac. Sci. Technol. 13, 721 (1976).
[58]T. S. Stein, W. E. Kauppila, and L. O. Roellig, Rev. Sci. Instrum. 45, 951 (1974).
[59]D. E. Golden, Rev. Sci. Instrum. 44, 1339 (1973).
[60]S. Golden and I. R. Epstein, Phys. Rev. A 10, 761 (1974).
[61]D. M. Schrader (private communication).
[62]T. F. O'Malley, Phys. Rev. 130, 1020 (1963).
[63]T. F. O'Malley, Phys. Lett. 54A, 196 (1977).
[64]P. F. Naccache and M. R. C. McDowell, J. Phys. B 7, 2203 (1974).
[65]R. W. Crompton, M. T. Elford, and A. G. Robertson, Aust. J. Phys. 23, 667 (1970).
[66]Y. K. Ho, J. Phys. B 10, L149 (1977).
[67]B. A. P. Page, J. Phys. B 8, 2486 (1975).
[68]R. J. Drachman, J. Phys. B 5, L30 (1972).
[69]C. L. Pekeris, Phys. Rev. 115, 1216 (1959).
[70]A. G. Robertson, J. Phys. B 5, 648 (1972).
[71]R. P. McEachran, A. G. Ryman, and A. D. Stauffer, J. Phys. B 11, 551 (1978).
[72]S. Hara and P. A. Fraser, J. Phys. B 8, 219 (1975).
[73]R. P. McEachran, A. G. Ryman, and A. D. Stauffer, J. Phys. B 12, 1031 (1979).